

Title: Progress in Understanding North American Monsoon Using a Climate Model

Authors: Ehsan Erfani^{1*} and David Mitchell¹

Affiliation: ¹Desert Research Institute, Reno, Nevada, USA

**Corresponding author email: Ehsan.Erfani@dri.edu*

Keywords: Climate modeling, monsoon, WRF model, Air-Sea interaction, North American monsoon, precipitation, Gulf of California, sea surface temperature, boundary layer, low-level jet

This is a preprint version of a paper that has been peer-reviewed and accepted for publication in the Academia Letters.

Paper doi: <https://doi.org/10.20935/AL463>

Paper citation: Erfani, E., Mitchell, D. (2021). Progress in understanding North American Monsoon Using a Climate Model. Academia Letters, Article 463

Progress in Understanding North American Monsoon Using a Climate Model

Ehsan Erfani¹ and David L. Mitchell¹

¹*Desert Research Institute, Reno, Nevada, USA*

**Corresponding author email: Ehsan.Erfani@dri.edu*

ABSTRACT

The North American Monsoon is a seasonal shift in the large-scale circulation that supplies 60-80% of annual rainfall in northwestern Mexico and 30-40% in the US southwest. Regional climate models have shown that summer precipitation prediction over North America is the poorest in the Monsoon region. Most climate models do not account for a crucial mechanism of Monsoon: the boundary layer inversion over the Gulf of California controls the low-level moisture transport. To investigate this mechanism, a set of carefully designed simulations of a regional climate model is used to investigate the dependence of Monsoon precipitation on sea surface temperature (SST) in the Gulf. The results are consistent with enhanced observations from a field campaign and show that warmer Gulf SSTs tend to weaken boundary layer inversion and enhance low-level moisture flux, and as a result, more Monsoon precipitation occurs. This highlights the necessity for climate models to implement the mentioned mechanism.

1. Introduction

North American Monsoon (hereafter, Monsoon) is important in determining the hydrological cycle in the US Southwest (Douglas et al., 1993) and synoptic-scale circulations over North America (Ordoñez et al., 2019). Over the past decades, various studies showed that numerous atmospheric and oceanic features (such as MJO, ENSO) and multiple moisture sources (such as the Pacific Ocean, Gulf of California, and the Gulf of Mexico) affect NAM [see Adams and Comrie (1997) for a review of those effects]; yet many of the NAM features, including climate prediction of precipitation by models, are still not well understood (Mearns et al., 2012).

Mitchell et al. (2002) showed a correlation between the sea surface temperature (SST) in the Gulf of California (hereafter, Gulf) and Monsoon precipitation, but the underlying mechanism was uncertain. Using observations, Erfani and Mitchell (2014) and Erfani (2016) demonstrated a local-scale mechanism of Monsoon: before Monsoon onset, the strong low-level temperature inversion over the Gulf prevents the mixing between the near-surface moist air in the marine boundary layer (MBL) and the dry air in the free troposphere (FT). This inversion weakens with an increase in Gulf SST, allowing the trapped moist air in the MBL to rise to FT. This leads to a deep, moist layer that can be moved to the Monsoon region by low-level jets.

Most reanalysis datasets such as the National Center for Environment Prediction (NCEP) Department of Energy (DOE) (Kanamitsu et al., 2002) have a coarse horizontal resolution (e.g. 1° or larger) that underestimates Gulf SSTs by 2°C or more (Erfani, 2016). Those reanalysis data are commonly used in climate models as the bottom boundary, which then correspond to insufficient local processes needed to correctly simulate Monsoon precipitation. To better understand this issue, we use Weather Research and Forecasting (WRF) and perform multiple experiments to capture the mechanisms of Monsoon in climate models.

2. Methodology

To investigate the strength of the local-scale mechanism, the WRF model, version 3.4.1 (Bruyere et al. 2010) was used in this research for the period of 8-17 July 2004. We selected a 10-day period of simulation because we are focused on the prediction of a synoptic-scale phenomenon, Monsoon onset, that does not exceed longer than 10 days. Also, the forecast skill would decrease significantly in WRF if the run period was longer. Our model can capture the effect of SST on the atmosphere because we prescribed SST in the WRF, and the atmosphere responds to the SST within a few hours (Bruyere et al. 2010).

Two nested domains were used: the main domain has a horizontal resolution of 30 km and covers Mexico, Southern U.S., and adjacent water bodies, whereas the nested domain has a horizontal resolution of 10km and covers the Monsoon region (Fig. 1). For initial and boundary conditions, the 6-hourly NCEP-DOE reanalysis dataset is used with a horizontal resolution of 2.5° and with 28 vertical levels. To test the effect of SST, three SST scenarios were defined as bottom boundary (Fig. 2): 1) *control* run used reanalysis SSTs; 2) Prescribed “*cold-SST*” run is defined by modifying Gulf SST so that northern Gulf SST = 26°C and southern Gulf SST = 28°C; 3) Prescribed “*warm-SST*” run is defined by making the whole Gulf SST being 30°C. The latter run is very similar to Advanced Very High-Resolution Radiometer (AVHRR) satellite data (Fig. 2c). The danger of using coarse SST data in climate models is depicted in Fig. 2d: NCEP-DOE data cannot resolve the Gulf and interpolate SST from the eastern Pacific, which is relatively cold.

For each SST scenario, we performed 8 sensitivity runs with different combinations of physics parameterizations to verify the robustness of the SST effect on Monsoon precipitation. A total of 24 simulations were performed. See Erfani (2016) for more details on the modeling descriptions. The results are compared with enhanced observations from the North American Monsoon Experiment (NAME) field campaign (Higgins et al., 2006), including High-resolution radiosonde and rain-gauge networks covering most of the Monsoon region.

3. Results

All WRF experiments capture the tropical cyclone that passed the southern Gulf that induced strong along-Gulf moisture flux (Gulf surge) with an across-Gulf component over the land during the 2004 monsoon onset (Fig. 3). Also, warm-SST run tends to produce stronger moisture flux than cold-SST run. In particular, a 40% increase in moisture flux is seen in the northern Gulf. The minor gulf surge on 9-10 July is seen in both model results and observations, and the major gulf surge on 13-14 July is associated with a higher mixing ratio and lower temperature in both MBL and free troposphere (Figs. 4 and 5). In agreement with the analysis of moisture flux, throughout the simulations, the warm-SST run produces warmer and moister MBL air than does cold-SST run (Figs. 4 and 5).

Simulations before NAM onset produced a shallow MBL with strong inversion that traps moisture in MBL and therefore generates a moist MBL and a dry free troposphere (Fig. 6). During NAM, inversion weakens and as a result, the free troposphere becomes more humid. Compared to WRF with cold SST, WRF with warm SST leads to warmer air temperature in MBL, and consequently weaker inversion, and more low-level (from the surface to 800 hPa) moisture. The extra moisture is transported to northwestern Mexico and southern Arizona (Fig. 3) and causes 30% more precipitation over southern Arizona and the mountain foothills of northwestern Mexico (Fig. 7).

Note that WRF enhanced the precipitation over the foothills of SMO (from latitude 23 to 29 °N) due to intensified across-Gulf wind component, and over eastern AZ due to intensified along-Gulf wind component.

Here, we only showed the results for the inner domain, but a similar pattern is seen in the outer domain, with slight differences in the strength of moisture and precipitation. Moreover, we only presented the mean of 8 ensemble members for each of the three WRF scenarios, but each member also represents the overall pattern. Although the warm-SST run generates a weaker MBL inversion than does cold-SST, all three WRF runs simulate an inversion that is stronger than observations (Fig. 6). This causes colder and drier air above MBL and less precipitation in WRF runs when compared to observations (Figs. 4-7). Reducing this bias is beyond the scope of this study, but it highlights an opportunity for WRF developers to improve their boundary layer parameterization over North America. We speculate that with such improvement, the effect of Gulf SST on NAM precipitation would be even stronger. The purpose of this study is not quantifying the biases and determining their sources; rather, we are focused on the isolation of the effect of the Gulf of California SST on NAM precipitation. For this reason, we mainly compared cold-SST and warm-SST runs. No nudging was used in this study, so the current difference between models and observations is not surprising.

4. Conclusions

To test the local-scale mechanism of Monsoon, the WRF model was used to investigate the effect of Gulf SST on precipitation, moisture flux, and vertical profiles of mixing ratio and air temperature during the Monsoon onset and the passage of gulf surge from 8 to 17 July 2004. These analyses showed when Gulf SST exceeds a threshold of 29°C, it leads to a 40% increase in low-level moisture flux in the Northern Gulf and a 30% increase in Arizona precipitation. The mechanism for such results is that the increase in Gulf SST leads to the weakening of the MBL temperature inversion, and consequently corresponds to the mixing of MBL moist air with FT that is then transported over southern Arizona and northwestern Mexico, and causes enhanced Monsoon precipitation. This study complements previous observations (Erfani and Mitchell, 2014) and modeling experiments (Erfani, 2016; Pascale et al., 2019), and further, sheds light on the local-scale processes controlling Monsoon precipitation in climate models.

Our study is novel and specific for the NAM because we showed the effect of the Gulf of California, which is such a small body of water, but its SST is ~ 10°C warmer than the adjacent Pacific SST. This significant SST difference affects the MBL inversion and moisture content and therefore NAM precipitation. However, the mentioned SST difference is not captured in many reanalysis datasets and global climate models that use a resolution of 100km or larger. As a result, using such datasets/models as initial/boundary conditions or using coarse resolution would lead to underestimation of precipitation as shown by other studies (e.g. Mearns et al., 2012)

Since NAM precipitation is the main source of flash floods in arid/semiarid Southwestern U.S. (Mitchell et al., 2002; Yang et al., 2019), the improvement of the NAM precipitation forecast will significantly reduce the societal and environmental impacts of such hazards. Future work will include numerical experiments with multiple climate models during various Monsoon seasons.

Data Availability Statement

The radiosonde and precipitation datasets related to the NAME field campaign are available from the NCAR/EOL website at <https://data.eol.ucar.edu/project/7> (NCAR/EOL is sponsored by the National Science Foundation). AVHRR SST can be downloaded from <https://search.earthdata.nasa.gov/search?fi=AVHRR>. NCEP-DOE reanalysis datasets are publicly available at <https://psl.noaa.gov/data/gridded/data.ncep.reanalysis2.html>. WRF model is publicly accessible from <https://www.mmm.ucar.edu/models/wrf>.

References

- Adams, D. K., and A. C. Comrie (1997): The North American Monsoon, *Bull. Am. Meteorol. Soc.*, **78**, 2197-2214.
- Bruyere, C., et al. (2010), Weather Research and Forecasting ARW version 3 modeling system user's guide. National Center for Atmospheric Research, 312 pp.
- Douglas, M., R. Madox, and K. Howard (1993), The Mexican monsoon. *J. Climate*, **6**, 1665-1677.
- Higgins, R., et al. (2006), The NAME 2004 field campaign and modeling strategy, *Bull. Am. Meteorol. Soc.*, **87**, 79-94.
- Erfani, E., and D. Mitchell (2014), A partial mechanistic understanding of the North American monsoon, *J. Geophys. Res. Atmos.*, **119**, 13096-13115. <https://doi.org/10.1002/2014JD022038>
- Erfani, E. (2016), A partial mechanistic understanding of North American Monsoon and microphysical properties of ice particles, University of Nevada-Reno, Ph.D. Dissertation, 229 pp, <http://doi.org/10.13140/RG.2.2.26526.79685>
- Kanamitsu, M., et al. (2002), NCEP-DOE AMIP-II Reanalysis (R-2). *Bull. Amer. Meteor. Soc.*, **83**, 1631-1643.
- Mearns, L., et al. (2012), The North American Regional Climate Change Assessment Program: Overview of Phase I Results. *Bull. Amer. Meteor. Soc.*, **93**, 1337-1362.
- Mitchell, D., D. Ivanova, R. Rabin, T. Brown, and K. Redmond (2002), Gulf of California sea surface temperatures and the North American monsoon: Mechanistic implications from observations. *J. Climate*, **15**, 2261- 2281.
- Ordoñez, P., et al. (2019): Climatological moisture sources for the Western North American Monsoon through a Lagrangian approach: their influence on precipitation intensity. *Earth System Dynamics*, **10.1**.
- Pascale, S., et al. (2019): Current and Future Variations of the Monsoons of the Americas in a Warming Climate. *Current Climate Change Reports*, **5.3**, 125-144.
- Yang, L., J. Smith, M. L. Baeck, and E. Morin (2019): Flash flooding in arid/semiarid regions: climatological analyses of flood-producing storms in central Arizona during the North American monsoon. *J. Hydrometeor.*, **20(7)**, 1449-1471.

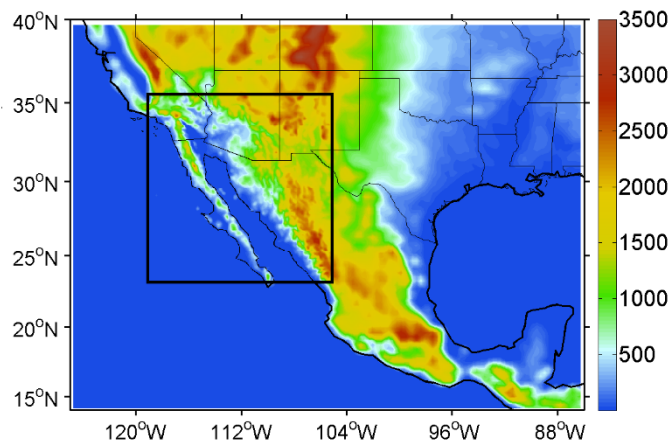


Fig. 1. Model domains in the WRF simulations: The outer (inner) domain with a resolution of 30 km (10 km) is shown by the outer (inner) black rectangle. Also shown is the topography of the region.

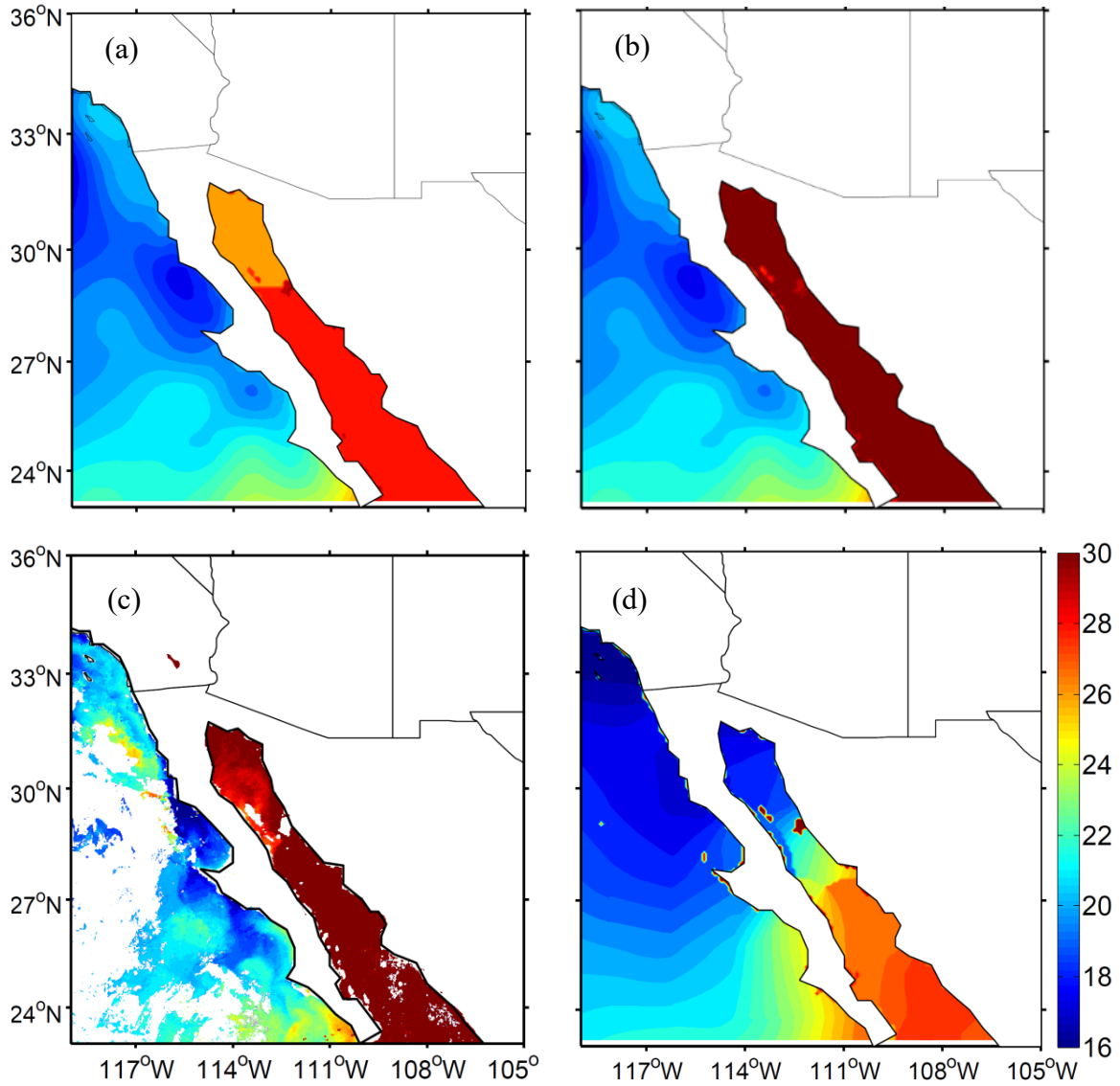


Fig. 2. (a) Prescribed "cold-SST", and (b) prescribed "warm-SST" as WRF bottom boundary. (c) AVHRR satellite SST averaged from 8 to 17 July 2004. The lack of data in some regions is due to overcast conditions. (d) NCEP-DOE SST interpolated to WRF grid points and averaged from 8 to 17 July 2004.

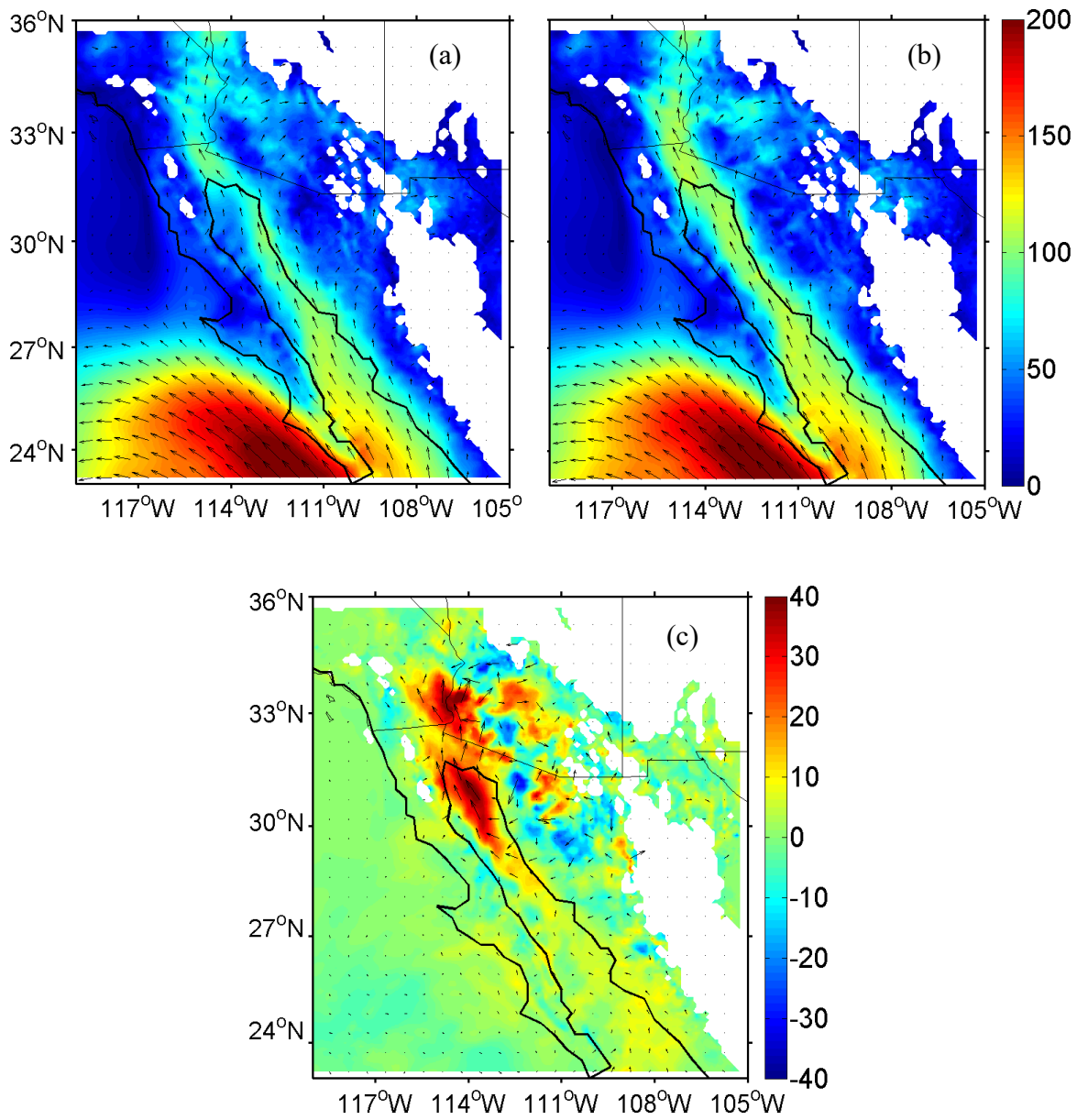


Fig. 3. WRF Moisture flux (in units of $\text{g m kg}^{-1} \text{s}^{-1}$) integrated from surface to 850 hPa on 14 July 2004 for a) ensemble-mean warm-SST model and b) ensemble-mean cold-SST model. (c) The percent difference between (a) and (b).

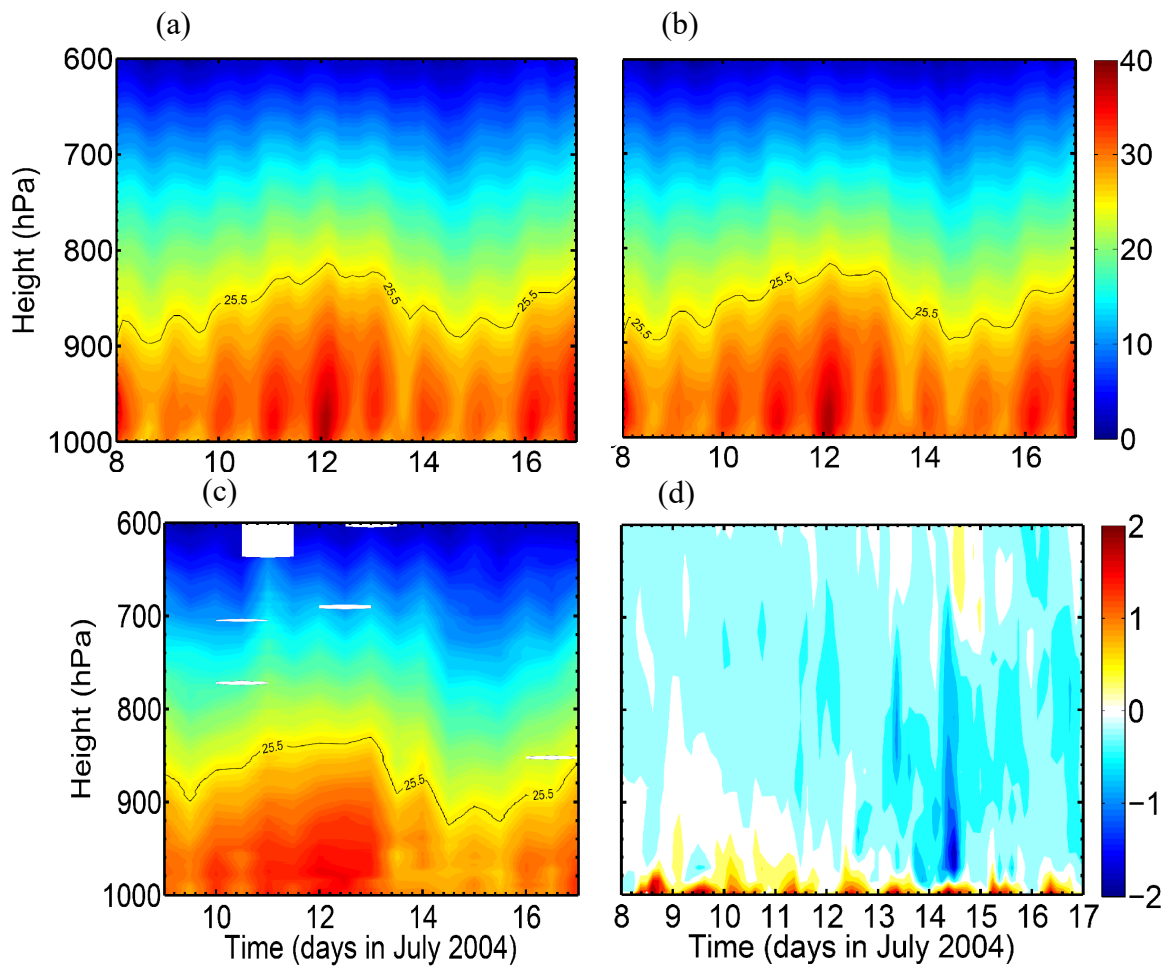


Fig. 4. Time series of the vertical profile of air temperature over Northern Gulf from (a) ensemble-mean cold-SST model, (b) ensemble-mean warm-SST model, and (c) observations. (d) The temperature difference between (a) and (b).

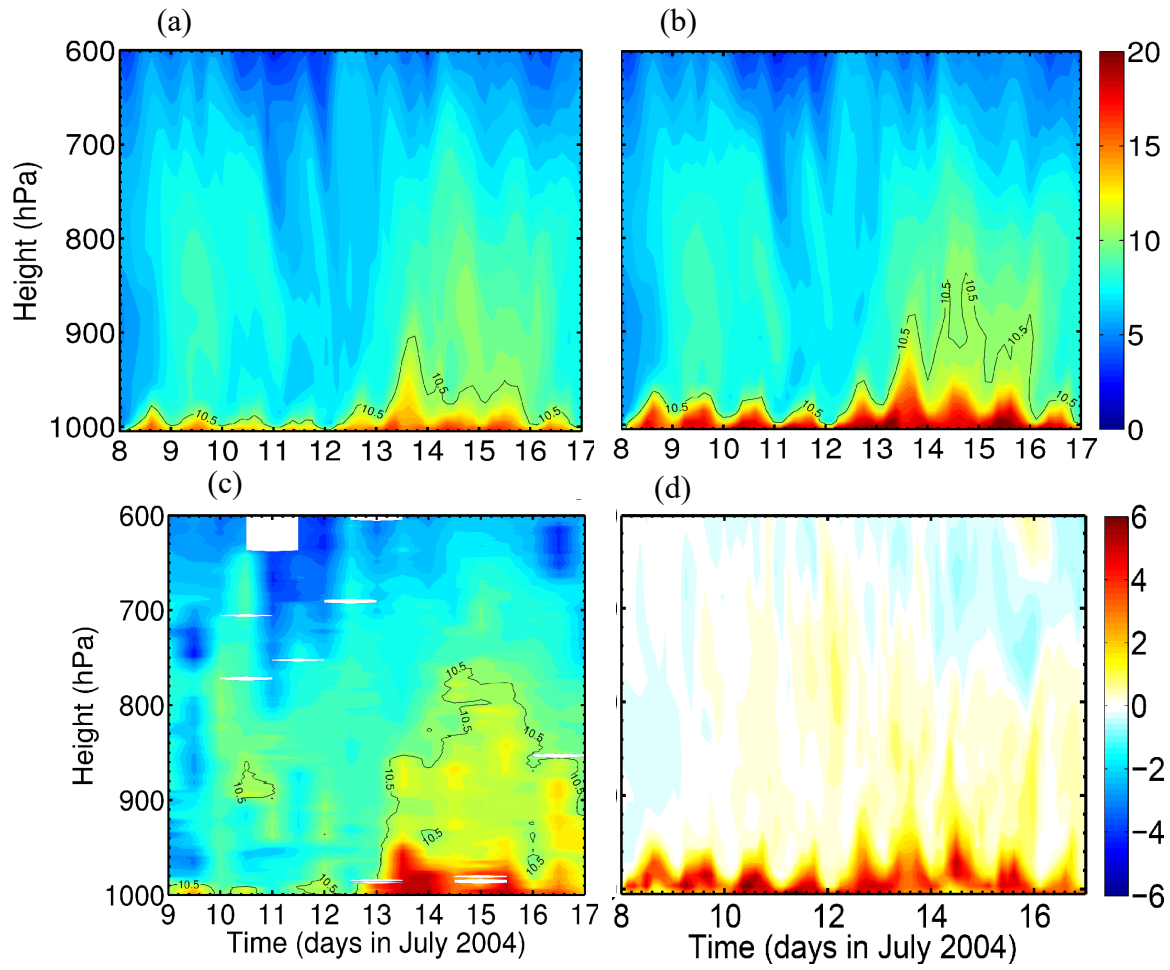


Fig. 5. As in Fig. 4, but for mixing ratio.

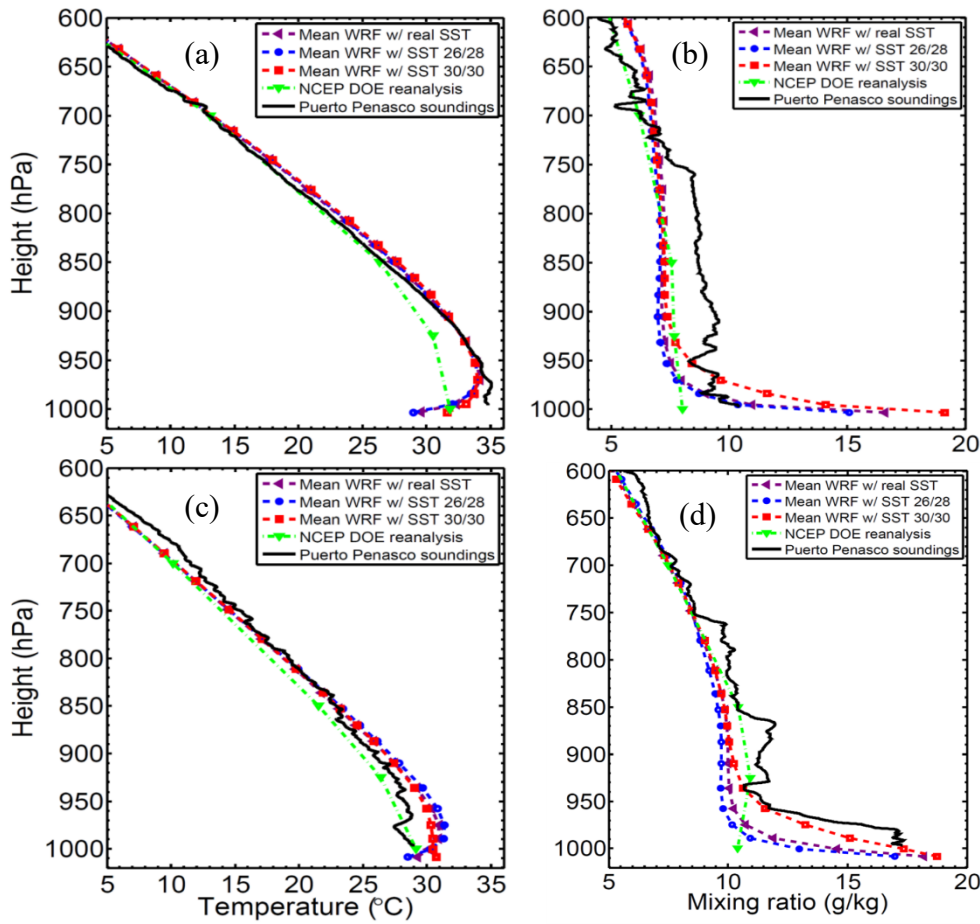


Fig. 6 (a) Vertical profile of air temperature averaged on 12 July 2004. (b) As in (a), but for mixing ratio. (c) As in (a) but averaged on 14 July 2004. (d) As in (c) but for mixing ratio. Model results are averaged for grid points in northern GC, whereas soundings are from Puerto Penasco, MX (closest available soundings). All modeling results are ensemble-mean, with “WRF w/ real SST” as *control*, “WRF w/ SST 26/26” as *cold-SST*, and “WRF w/ SST 30/30” as *warm-SST*. NCEP-DOE reanalysis is also shown.

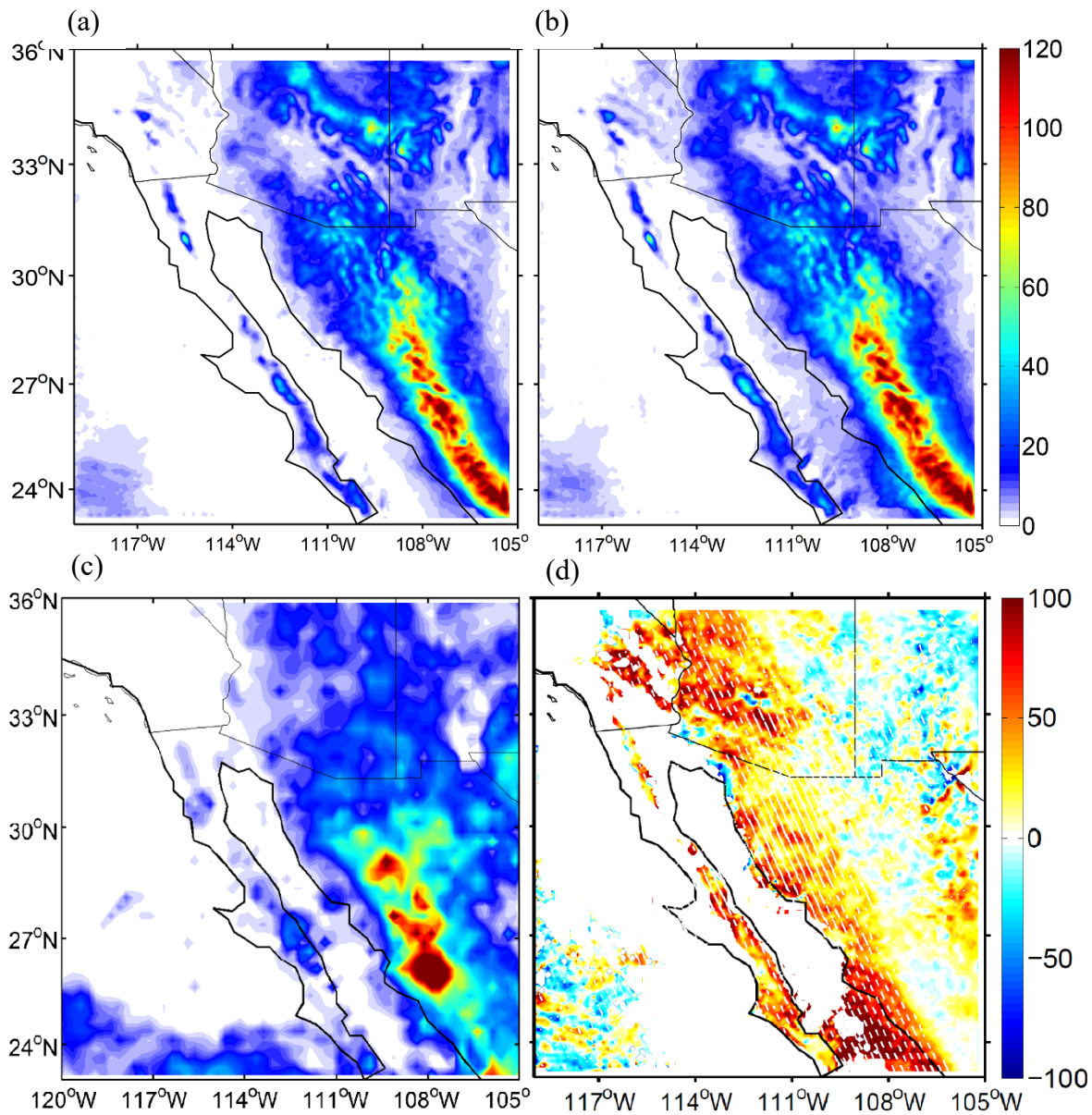


Fig. 7. Accumulated precipitation from 8 to 17 July 2004 for (a) ensemble-mean cold-SST model, (b) ensemble-mean warm-SST model, and (c) observations. (d) The percent difference between (a) and (b). Hatched regions show statistically significant results.